

Membrane fluidity of halophilic ectoine-secreting bacteria related to osmotic and thermal treatment

Sven Bergmann · Florian David · Wiebke Clark ·
Christoph Wittmann · Rainer Krull

Received: 8 February 2013 / Accepted: 12 April 2013
© Springer-Verlag Berlin Heidelberg 2013

Abstract In response to sudden decrease in osmotic pressure, halophilic microorganisms secrete their accumulated osmolytes. This specific stress response, combined with physiochemical responses to the altered environment, influence the membrane properties and integrity of cells, with consequent effects on growth and yields in bioprocesses, such as bacterial milking. The aim of this study was to investigate changes in membrane fluidity and integrity induced by environmental stress in ectoine-secreting organisms. The halophilic ectoine-producing strains *Alkalibacillus haloalkaliphilus* and *Chromohalobacter salexigens* were treated hypo- and hyper-osmotically at several temperatures. The steady-state anisotropy of fluorescently labeled cells was measured, and membrane integrity assessed by flow cytometry and ectoine distribution. Strong osmotic downshocks slightly increased the fluidity of the bacterial membranes. As the temperature increased, the increasing membrane fluidity encouraged more ectoine release under the same osmotic shock conditions. On the other hand, combined shock treatments increased the number of disintegrated cells. From the ectoine release and membrane integrity measurements under coupled thermal and osmotic shock conditions, we could optimize the secretion conditions for both bacteria.

Keywords Membrane fluidity · Steady-state fluorescence anisotropy · Osmotic and thermal shock · Ectoine release · Halophile bacteria

Abbreviations

DMSO	Dimethyl sulfoxide
DPH	1,6-Diphenyl-1,3,5-hexatriene
<i>I</i>	Fluorescence emission intensity
PI	Propidium iodide
r_{DPH}	Steady-state anisotropy
T_{m}	Phase transition temperature

Introduction

Halophilic microorganisms accumulate compatible solutes such as ectoine to protect their intracellular compounds against environmental stress, thereby improving their reproductive capacity. Ectoine also fluidizes the lipid bilayers by increasing the mobility of the lipid head groups, which may be advantageous for the cell membranes against extreme physiological conditions [1].

On the other hand, halophiles secrete these compatible solutes under hypo-osmotic stress to maintain cellular stability [2]. Such changes in environmental conditions will primarily affect the cellular membrane, which is directly exposed to the threat. Stressors affect the physical properties and composition of the membrane, as well as transport mechanisms and turgor, with subsequent adverse effects on proliferation and survival. Beside osmosensing and osmoregulation (via accumulation of compatible solutes), halotolerant and halophilic microorganisms modify their membrane proteins and lipid compositions under osmotic stress, thereby altering the membrane phase properties [3]. As compatible solutes are rapidly discharged through mechanosensitive channels, changes in turgor pressure and ion transport influence the membrane microviscosity, in turn affecting ectoine release. In *Saccharomyces cerevisiae*,

S. Bergmann · F. David · W. Clark · C. Wittmann ·
R. Krull (✉)
Institute of Biochemical Engineering, Technische Universität
Braunschweig, Gaußstraße 17, 38106 Braunschweig, Germany
e-mail: r.krull@tu-braunschweig.de

S. Bergmann
e-mail: s.bergmann@tu-braunschweig.de

fluidity of cell membrane (microviscosity) and cell viability is strongly affected by osmotic and thermal treatment [4, 5]. Membrane fluidity of *Escherichia coli* cells decreases under increasing osmotic pressure, leading to cell death at some critical value [6]. Membrane fluidity can be determined by measuring the steady-state anisotropy r of fluorescently-labeled cell membranes. At the membrane phase transition temperature T_m , the anisotropy changes dramatically [7]. Such changes are characteristic of gel to liquid-crystalline phase transitions, and reflect increases in relative mobility of the membrane lipid bilayer. To observe membrane fluidity and phase transitions, cells may be labeled with the fluorescent dye 1,6-diphenyl-1,3,5-hexatriene (DPH) [8]. DPH labels the lipophilic part of membrane compounds and penetrates viable cell membranes, extracted biological membranes and liposomes. At low concentrations, DPH preserves the morphology of membrane structures [9, 10], allowing in vivo measurements of stress responses and interpretation of cell membrane physiology [11]. Using this technique, the cell membranes of many organisms, including *Zygosaccharomyces rouxii*, *Shewanella gelidimarina*, *Bacillus subtilis*, and *Lactobacillus bulgaricus*, have been shown to become more rigid on salty or high osmolality substrates [12–15]. DPH has also been applied in membrane fluidity measurements of halophilic archaea exposed to alcohols [16]. Another fluorescence intensity approach detects the amount of intercalated DPH within the bacterial membranes using single cell technique, enabling assessment of membrane fluidity changes without considering the polarization of DPH molecules [17]. Besides fluidity, the integrity of the membrane is a crucial measure, since secreted ectoine must be differentiated from leakage. To assess membrane integrity, the cells are exposed to the fluorochrome propidium iodide (PI). PI penetrates into injured cells and allows, in combination with a green nucleic acid probe (e.g., SYBR Green or Syto 9), the quantification of intact cells and those with reduced integrity using flow cytometry [18, 19].

In this work, the little investigated halophile bacteria *Alkalibacillus haloalkaliphilus* was subjected to hyper- and hypo-osmotic shocks at different temperatures (ranging from 20 to 60 °C). The ectoine release behavior, membrane fluidity and integrity were assessed. Membrane fluidity was determined from fluorescence steady-state anisotropy of DPH-labeled cells. To detect cells that had been injured by osmotic downshock or heating, the numbers of intact and disintegrated cells were determined by flow cytometry of cells stained with Syto 9 and PI. In former study, the optimum ectoine concentration by *A. haloalkaliphilus* (about 200 mg L⁻¹) was obtained in alkaline nutrient broth containing 132 g L⁻¹ NaCl after 11 h cultivation [20]. For comparisons, the extensively studied ectoine producer

Chromohalobacter salexigens [21] was treated and analyzed in the same way.

Materials and methods

Microorganisms

Alkalibacillus haloalkaliphilus strain DSM 5271^T and *C. salexigens* strain DSM 3043^T were obtained from the German Collection of Microorganisms and Cell Cultures (DSMZ, Germany) as vacuum dried cultures.

Cultivation

Cells were grown in Nutrient Broth containing 5.0 g L⁻¹ soy peptone, 3.0 g L⁻¹ meat extract (Fluka, Sigma-Aldrich, Germany) and 132 g L⁻¹ sodium chloride (NaCl). The pH value was adjusted to 7.0 using 1 M NaOH. *A. haloalkaliphilus* cultures were maintained at pH 8.9 by addition of 0.1 M sodium sesquicarbonate buffer before inoculation. All other chemicals were purchased from Sigma-Aldrich (Germany), Merck (Darmstadt, Germany) or Roth (Karlsruhe, Germany) with analytical grade. All pre-cultures and experiments were performed in baffled shake flasks (250 mL) containing 20-mL medium at 37 °C, 130 min⁻¹ and 50 mm shaking diameter (CERTOMAT BS-1, Sartorius Stedim, Göttingen, Germany). All experimental flasks were inoculated with exponentially growing cells at optical density of ≈ 0.9 at 660 nm (OD₆₆₀) for *A. haloalkaliphilus* and 600 nm (OD₆₀₀) for *C. salexigens*.

Quantification of cell concentration

Cell concentration was measured by optical density (OD₆₆₀ and OD₆₀₀ for *A. haloalkaliphilus* and *C. salexigens*, respectively) using a UV-Vis spectrometer (Genesys 10S, Thermo Electron Scientific, Madison, WI, USA) and semi-micro cuvettes (PS-1.5 mL, Brand, Wertheim, Germany).

Sample preparation and osmotic treatment

Samples were centrifuged at 1,500× g at room temperature for 8 min and washed twice in saline buffer containing 132 g L⁻¹ NaCl and 0.1 M sodium sesquicarbonate buffer (pH 8.9; *A. haloalkaliphilus*) or 0.1 M sodium phosphate buffer (pH 7.2; *C. salexigens*), to avoid osmotic cell damage. Subsequently, the carefully washed cell pellets were resuspended in saline treatment solutions containing 20, 40, 60, 80, 100, 132, or 145 g L⁻¹ NaCl and a final concentration of 0.1 M sodium sesquicarbonate buffer (pH 8.9; *A. haloalkaliphilus*) or 0.1 M sodium phosphate buffer (pH 7.2; *C. salexigens*). Each cell solution was diluted to

$OD_{600} = 0.1$ (Novaspec III, Amersham Bioscience, Freiburg, Germany) in the corresponding saline treatment solution.

Ectoine release

Ectoine secretion under hypo- and hyper-osmotic conditions was investigated in duplicate for several coupled thermal and osmotic treatments. For this measurement, 1 mL aliquots of culture broth ($OD = 0.9$) were centrifuged at $1,500\times g$ at room temperature. The supernatant was removed and the pellet was incubated for 5 min at 20, 40, or 60 °C. Subsequently, 1 mL of saline treatment solution pre-heated at the specific temperature, was added and softly mixed with a pipette. After 5 min further incubation at the specified temperature, the intra- and extracellular ectoine concentration was quantified.

Quantification of ectoine

Samples were centrifuged for 5 min at $21,100\times g$ at room temperature. Intracellular ectoine was quantified by HPLC by a recently described method, based on extraction from lyophilized cell pellets proposed by Bligh and Dyer [21, 22]. Briefly, 120 mg of polished glass beads (diameter 35–45 μm , Worf, Mainz, Germany) and 500 μL of a methanol/chloroform/water solution (volume ratio 10:5:4) were added to the pellets and treated in a high speed homogenizer (FastPrep-24, MP Biomedicals, Solo, Ohio, United States) for 4 min at 4.0 m s^{-1} . Subsequently, 130 μL chloroform and 130 μL H_2O were added, followed again by 1 min homogenization at 4.0 m s^{-1} . The resulting two-phase system was centrifuged for 5 min at $21,100\times g$ at room temperature. Ectoine was measured in the aqueous phase using a HPLC (LaChrom system, Merck-Hitachi, Darmstadt, Germany) equipped with a NucleoSIL 250 \times 5.6 C18 AQ-plus column (Knauer, Berlin, Germany). The eluent was a phosphate buffer containing 0.8 mM KH_2PO_4 and 6 mM Na_2HPO_4 (pH 7.6). UV detection was performed at 220 nm and an isocratic flow of 1.0 mL min^{-1} at 40 °C was used. The retention time of ectoine was approximately 3.7 min. Extracellular ectoine concentration was measured in the filtered supernatant (0.2 μm pore size, Minisart, Sartorius Stedim, Goettingen, Germany).

Membrane labeling

A 2 mL aliquot of cell solution (diluted to $OD_{600} = 0.1$) was labeled with fluorescence marker DPH (Sigma Aldrich, Germany) by adding 4.8 mM DPH stock solution (in tetrahydrofuran). The solution was then incubated with slow shaking (350 min^{-1}) at 37 °C (growth temperature) (Thermomixer comfort, Eppendorf, Germany) in the dark,

allowing the probe to incorporate into the bacterial membrane. Cells suspensions were equivalently stained in quartz cuvettes at 37 °C (incubated in a cuvette holder) in method alignment experiments.

Steady-state anisotropy measurements

Fluorescence anisotropy was first described by the equation of Perrin [23], who proposed that

$$\frac{r_0}{r} = 1 + \frac{\tau}{\theta}, \quad (1)$$

where r_0 is the fundamental anisotropy in the absence of rotational diffusion, r is the measured anisotropy, τ is the fluorescence lifetime and θ is the rotational correlation time of the fluorophore, related to the dynamic microviscosity of the membrane η and the hydrodynamic volume V of the rotating fluorescently labeled molecule as

$$\theta \sim \frac{\eta \times V}{R \times T}. \quad (2)$$

Here, R is the gas constant and T the absolute temperature. Generally, V , R , τ and r_0 are incorporated into a constant $K(r)$, yielding

$$\frac{1}{r} = \frac{1}{r_0} + K(r) \times \frac{T}{\eta}. \quad (3)$$

Equation (3) shows that the measured steady-state anisotropy r is proportional to the dynamic microviscosity η of the membrane. Moreover, steady-state anisotropy r and dynamic viscosity η are inversely proportional to the so-called membrane fluidity φ

$$r \sim \eta \sim \frac{1}{\varphi}. \quad (4)$$

Hence, using the DPH steady-state anisotropy parameter r_{DPH} provides qualitative information regarding the changes in microviscosity η_{DPH} and the related membrane fluidity φ_{DPH} in DPH-labeled areas of the cell membrane.

Steady-state anisotropy r_{DPH} was measured using a Quanta Master 40 fluorescence spectrometer (PTI, Birmingham, United States) equipped with a temperature-controlled cuvette holder and two Glan–Thompson polarizers arranged in L-format. Excitation and emission wavelengths were set to 358 and 428 nm, respectively. Slit widths of 10 nm were used. A 2 mL aliquot of unlabeled or stained samples ($OD_{600} = 0.1$) was transferred to a spectroscopic quartz cuvette (Type 101-QS, $10 \times 10\text{ mm}$, Helma Analytics, Muellheim, Germany) and placed into the pre-temperated cuvette holder. Single measurements were determined from scans collected at 20 s intervals at 37 °C. For combined thermal and osmotic treatment, the samples were temperature-adjusted to 20 °C and automatically heated to 60 °C at constant heating rate

(5 °C min⁻¹). Throughout heating, the vertical and horizontal fluorescence emission intensities were determined continuously. The software FelixGX (Version 4.1.1, PTI, USA) was used for data logging and measurement control. Subsequently, steady-state anisotropy r_{DPH} was calculated from the equation proposed by Lakowicz [7]:

$$r_{\text{DPH}} = \frac{(I_{\text{VV}} - I_{\text{VV}_0}) - G \times (I_{\text{VH}} - I_{\text{VH}_0})}{(I_{\text{VV}} - I_{\text{VV}_0}) + 2G \times (I_{\text{VH}} - I_{\text{VH}_0})}. \quad (5)$$

Here, I_{VV} and I_{VH} are the fluorescence emission intensities detected in the vertical (V) and horizontal (H) directions, respectively, relative to the vertical polarized excitation. The intensities are corrected by subtracting the intensity of unlabeled cells at particular salt concentrations (I_{VV_0} , I_{VH_0}). The grating factor G , defined as the ratio of the vertical and horizontal emitted intensities of horizontally polarized light ($G = I_{\text{HV}}/I_{\text{HH}}$), is specific for the sample setup. The obtained data were smoothed by a Fast Fourier Transform (FFT) filter with a cutoff frequency between 0.12 and 0.09 Hz.

Membrane integrity

To analyze the cell membrane integrity, cells were stained with the fluorescence dyes Syto 9 (Molecular probes, Eugene, USA) and PI (Sigma-Aldrich, Germany). Osmotic- and heat-treated cell solutions with $\text{OD}_{600} = 0.05$ were primary labeled by 2 min incubation in 3.34 μM Syto 9 (3.34 mM stock solution in DMSO). Subsequently, 7.5 μM PI (1.5 mM stock solution in DMSO) was added and the solution incubated for a further 5 min. During this incubation, PI penetrates cells with reduced membrane integrity, causing damaged cells to fluoresce more red. Single cell analysis was performed in a Quanta MPL flow cytometer (Beckman Coulter, Krefeld, Germany) equipped with a 488 nm argon laser. The side scatter (SS) signal was used as a trigger. Green (FL1) and red (FL3) fluorescence was detected through a dual long pass filter (525 nm) and a band pass filter (620 nm), respectively. Signals were logarithmically amplified and photomultiplier settings were adjusted to the used stains. For each measurement, 10,000 counts were sampled at 80–400 counts s⁻¹. To distinguish between intact cells from those with reduced membrane integrity, different mixtures of live (exponential phase) and heat treated cells (90 °C, 10 min) were measured similarly.

Results and discussion

Growth and ectoine accumulation

The investigated bacteria were cultivated in triplicate under the same nutrient and salinity conditions (NaCl

132 g L⁻¹). Cell growth began immediately and intracellular ectoine was accumulated from an early stage. *A.haloalkaliphilus* grew exponentially throughout the first 6 h of cultivation (Fig. 1a). The highest ectoine concentration (30 mg L⁻¹) was obtained at 8.5 h cultivation. By contrast, *C.salexigens* had accumulated 37 mg L⁻¹ of ectoine after 7 h cultivation, followed by a decrease (Fig. 1b). This species grew exponentially throughout the first 3.5 h of cultivation. Ectoine was not detected in the supernatant during the entire cultivation time.

DPH staining and method alignment on halophile organism

Steady-state anisotropy measurements using DPH were tailored to the requirements of *A. haloalkaliphilus* and *C. salexigens*. Suitable DPH concentrations and required

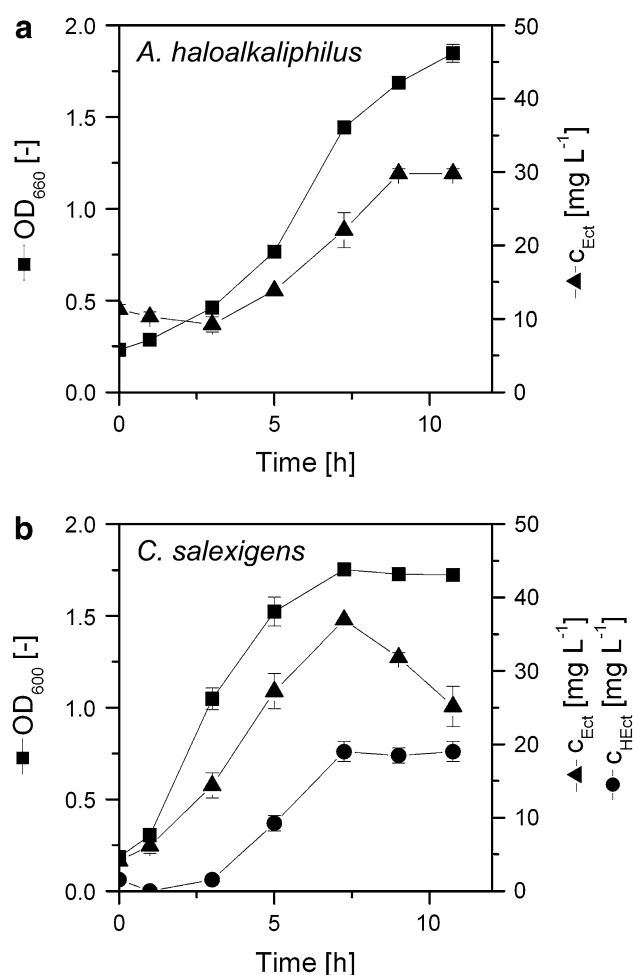
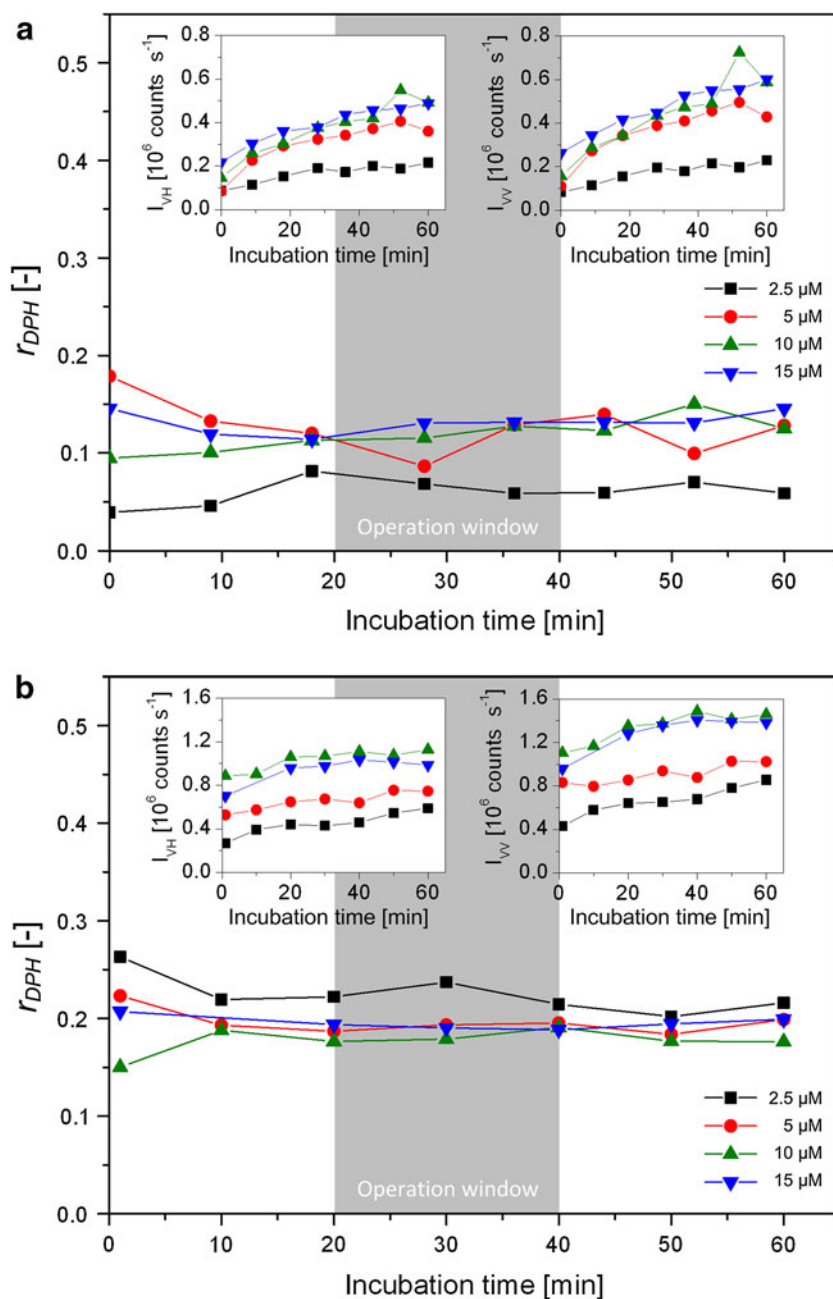


Fig. 1 Bacterial growth, determined by optical density (OD) at 600 or 660 nm (filled square), and intracellular ectoine (filled triangle) and hydroxyectoine concentrations in *A. haloalkaliphilus* (a) and *C. salexigens* (b) growing at 37 °C for 12 h in shake flasks containing nutrient broth with 132 g L⁻¹ NaCl. Extracellular ectoine was not detected

incubation times were determined from the results of Fig. 2. DPH was added to the cell suspensions at final concentrations of 2.5, 5, 10, and 15 μM and incubated for 60 min. The intensities were measured and the DPH steady-state anisotropy r_{DPH} was calculated by Eq. (5). After 60 min, the intensities of *A. haloalkaliphilus* cells continued to increase, indicating that labeling was not yet complete (Fig. 2a, insert). However, r_{DPH} remained constant between 20 and 45 min of incubation time due to the ratiometric analysis of intensities. Cells were labeled incompletely at dye concentrations below 10 μM , as revealed by constant low intensities after 30 min. Similar

labeling characteristics were observed of *C. salexigens* cells, but adequate measurements were obtained above 5 μM DPH (Fig. 2b). Therefore, further membrane fluidity measurements employed 10 and 5 μM for of *A. haloalkaliphilus* and *C. salexigens*, respectively. The dye was incubated for at least 20 min (maximum 40 min; see the gray shaded operation window in Fig. 2). From differences in the measured fluorescence intensities, as well as their progression, we infer that the strains possess different membrane properties. DPH penetrated the cell membrane of the gram-negative *C. salexigens* in higher concentrations than in *A. haloalkaliphilus*. The cell wall structure of

Fig. 2 Time-dependent stability of the steady-state anisotropy r_{DPH} and DPH labeling procedure, determined by varying the final DPH concentration. Experiment was conducted on exponential phase cells ($\text{OD} = 0.9$) of *A. haloalkaliphilus* (a) and *C. salexigens* (b) in nutrient broth containing 132 g L^{-1} NaCl at 37°C with shaking at 130 min^{-1} , washed twice and resuspended in saline buffer of the same NaCl content. Insets show the intensities I_{VH} and I_{VV}



A. haloalkaliphilus is that of a gram-positive organism [24], although the gram reaction is negative [25]. Therefore, the different fluorescence intensities might be related to the diverse cell wall structures and the number of hydrophobic membrane components.

Coupled thermal and osmotic treatment

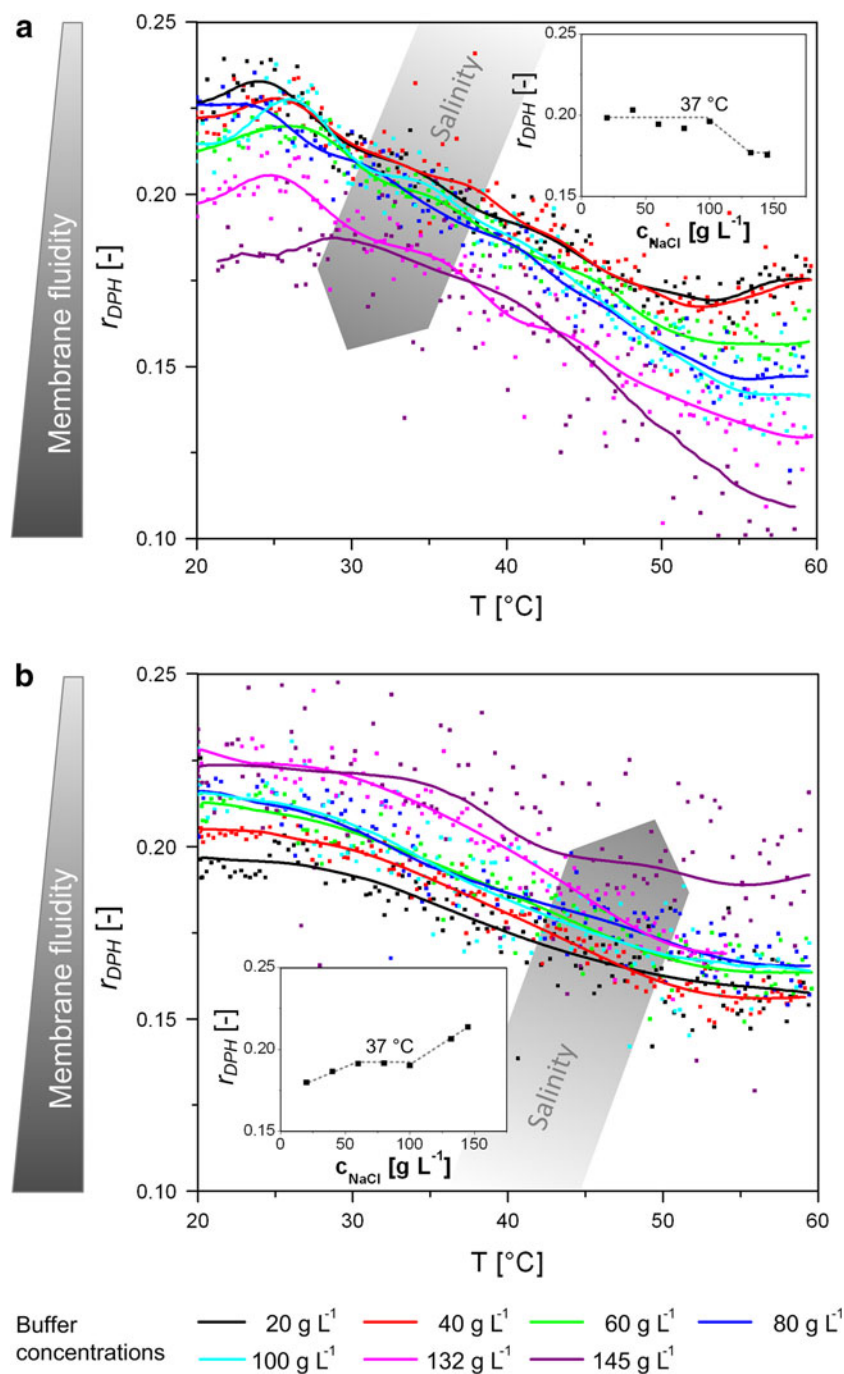
Halophilic bacteria can be forced to secrete their accumulated ectoine by osmotic treatment (bacterial milking)

[26, 27]. However, this process affects the fluidity and integrity of the cellular membrane. In addition, the membrane fluidity is temperature-dependent. Therefore, thermal and osmotic treatments were coupled in the following investigations.

Membrane fluidity

The lower the DPH steady-state anisotropy r_{DPH} , the higher the fluidity of the cell membrane φ_{DPH} (see Eq. 4). The

Fig. 3 Steady-state anisotropy r_{DPH} of *A. haloalkaliphilus* (a), and *C. salexigens* (b) cells labeled with DPH during combined osmo- and thermo-shock treatment from 20 to 60 °C. The cells were grown in nutrient broth containing 132 g L⁻¹ NaCl and resuspended in saline treatment solutions containing 20–145 g L⁻¹ NaCl. The gray bars along the ordinate (left) indicate the increase/decrease of membrane fluidity. The r_{DPH} response to increasing salinity is indicated by the gray arrows. Insets show the relationship between anisotropy and salinity at 37 °C



anisotropy profiles of cells subjected to osmotic shock between 20 and 60 °C (measured by temperature gradient) are shown in Fig. 3. As expected, the steady-state anisotropy r_{DPH} of both bacteria reduces with increasing temperature. During the investigated temperature range, anisotropy shift was higher in *A. haloalkaliphilus* (Fig. 3a) than in *C. salexigens* (Fig. 3b), indicating that *A. haloalkaliphilus* possesses the more flexible lipid membrane structure. For example, the high content of branched fatty acids in obligate alkaliphiles is thought to increase the membrane fluidity and permeability of alkaliphilic *Bacilli* [28, 29]. The membrane fluidity of *A. haloalkaliphilus* cells decreases and increases under hypo- and hyper-osmotic conditions, respectively (Fig. 3a). The opposite behavior is observed in *C. salexigens*. These behaviors are especially apparent in the anisotropy r_{DPH} versus salinity plots, obtained at 37 °C (growth temperature; Fig. 3, insets). Hypo-osmotic shocking of *A. haloalkaliphilus* (below 100 g L⁻¹ NaCl) induces an initial increase in r_{DPH} followed by stabilization as salt concentration is lowered further. The anisotropy of hypo-osmotically shocked *C. salexigens* cells, on the other hand, decreases from 0.21 to 0.19, remains constant between 60 and 100 g L⁻¹ NaCl and further declines below 40 g L⁻¹ NaCl. Increased anisotropy at higher osmolarities and comparable cultivation temperatures has been reported in other gram-positive and gram-negative microorganisms [13–15], although decreased r_{DPH} at hyper-osmotic conditions has, to date, been reported only in *Bradyrhizobium japonicum* [30]. High salt concentrations are expected to harden the bacterial membrane via cellular volume shrinkage, altered transport phenomena and changes in the hydration shell from the phospholipid bilayer, all of which likely affect the microviscosity of the cellular membrane. Ionic strength and pH reportedly influence the thickness of the diffuse layers around charged membrane surfaces [31], with consequent changes in steric configuration of phospholipids and, thus, in membrane fluidity. Since the phospholipid composition and the content of saturated and unsaturated fatty acids vary markedly between microorganisms, the effects of salt on membrane fluidity are not easily elucidated [3]. Vargas et al. [32] reported adaptive changes in the membrane lipid composition of *C. salexigens* following long-term salt stress. In particular, the cardiolipin content increased and the unsaturated fatty acids were converted to cyclopropane fatty acids, which are expected to stiffen the membrane. During hyper-osmotic treatment, the membrane fluidity showed the same behavior (Fig. 3b, inset). However, physical effects such as fatty acid modifications are characteristic of long-term adaptation. In response to hypo-osmotic shocks, halophiles open mechanosensitive channels to create large, nonselective pores through which cytoplasmic solutes are rapidly discharged. In this way, lysis is averted during osmotic downshock [33].

As the cell wall distorts, the membrane fluidity alters. In addition, lipid modifications within *C. salexigens* cell membranes might be attenuated by exogenous ectoine [32].

Effect on phase transition temperature

Beside cell membrane fluidity, the transition point between gel and liquid-crystalline state, defined as melting temperature or phase transition temperature T_m , can be determined. This characteristic value is strongly dependent on membrane composition. The bacterial cell membrane comprises several components, each with its own transition temperature. Here, as a benchmark for interpretation, T_m of the bacterial membrane is regarded as the midpoint of r_{DPH} decrease during melting. To this end, the anisotropy curves (Fig. 3) obtained by Fast Fourier Transform were integrated forwards and backwards from the highest and lowest anisotropy values ($r_{DPH,max}$ and $r_{DPH,min}$), respectively. If the resulting areas A were equal, their intercept, indicating the midpoint of phase transition and the T_m of the biological membranes, was estimated (see Fig. 4, inset).

In general, T_m is robust to osmotic stress (Fig. 4). The T_m of *C. salexigens* cells is constant over the investigated salinity range, indicating that the melting properties of the bacterial membrane are unaffected. Under high osmotic shocking (<60 g L⁻¹ NaCl), a change in the membrane lipid state of *A. haloalkaliphilus* cells appears; the cell membranes convert to a liquid-crystalline state at lower temperatures. As the salinity conditions alter from

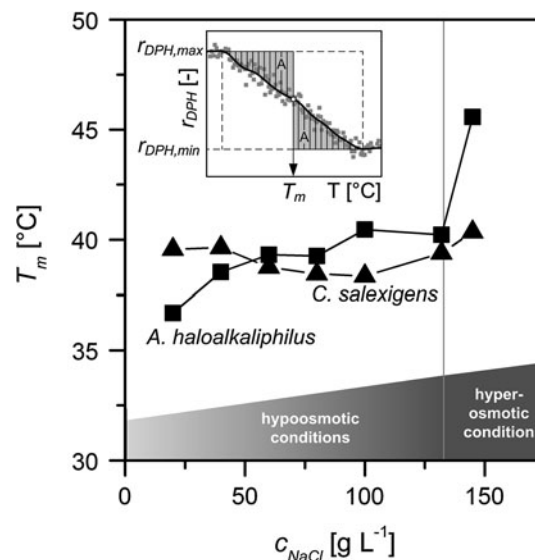


Fig. 4 Estimated midpoint phase transition temperature T_m under combined osmotic and thermal shock. $c_{NaCl} = 132$ g L⁻¹ is the salinity before osmotic treatment. *Inset* shows how the phase transition temperature T_m is determined from integrated anisotropy progression. *A. haloalkaliphilus* (filled square) and *C. salexigens* (filled triangle)

iso-osmotic ($132 \text{ g L}^{-1} \text{ NaCl}$) to hypo-osmotic ($20 \text{ g L}^{-1} \text{ NaCl}$) the T_m reduces by $4 \text{ }^\circ\text{C}$, representing a significant change in the fluidity characteristics. Such behavior has been reported in methylphosphatidic acid dispersions under high ionic strength (salt concentration) and alkaline conditions (pH), which alter the protonation of phosphate groups [31].

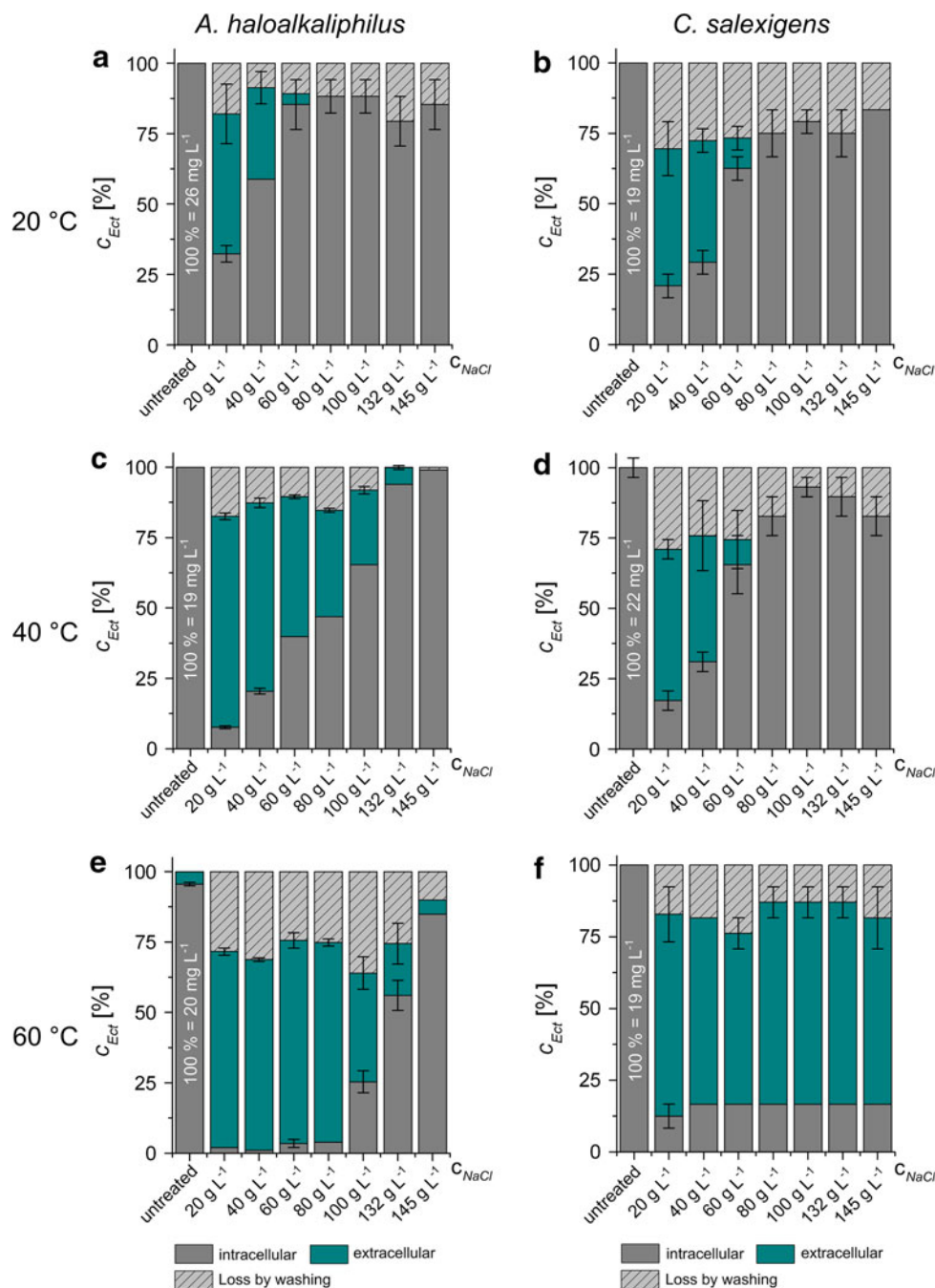
The large T_m increase exhibited by hyper-osmotically stressed *A. haloalkaliphilus* cells (at $145 \text{ g L}^{-1} \text{ NaCl}$) should be regarded with caution. This increase is related to the two transient phases appearing in the anisotropy plot

($145 \text{ g L}^{-1} \text{ NaCl}$) (c.f. Fig. 3a). Multiple transition phases reflect osmoadaptive changes in membrane composition, which should not occur within a mere 30 min of osmotic treatment.

Ectoine release

During hypo-osmotic treatment, the halophiles secrete compatible solutes, such as ectoine to avert against dehydration and hydration [2, 27]. As shown in Fig. 5, ectoine secretion is strongly affected by temperature and osmotic

Fig. 5 Ectoine release of untreated and hypo- or hyper-osmotically treated *A. haloalkaliphilus* (left column) and *C. salexigens* (right column) cells at $20 \text{ }^\circ\text{C}$ (a, b), $40 \text{ }^\circ\text{C}$ (c, d) and $60 \text{ }^\circ\text{C}$ (e, f). The cells were grown at $37 \text{ }^\circ\text{C}$ in nutrient broth containing $132 \text{ g L}^{-1} \text{ NaCl}$. Subsequently, the cells were shocked by resuspending in saline treatment solutions containing $20\text{--}145 \text{ g L}^{-1} \text{ NaCl}$. The pre-treatment intracellular ectoine concentration is provided in white font inside the column representing untreated cells



shocks. At 20 °C and low salt concentrations ($<60 \text{ g L}^{-1}$ NaCl), up to 50 % of the original intracellular concentration is secreted (Fig. 5a, b). At 40 °C, osmotic treatment is more effective in *A. haloalkaliphilus* than in *C. salexigens* cells. In the former, approximately 20 % ectoine had been released during downshock to 100 g L^{-1} NaCl. At 20 g L^{-1} NaCl, almost all the ectoine was found in the supernatant. By contrast, under hyper-osmotic conditions ($>130 \text{ g L}^{-1}$ NaCl), allowing for loss by washing, the intracellular solute concentration is increased (Fig. 5c). Washing is required for correct comparison of the ectoine release results with the steady-state anisotropy measurements. The ectoine release characteristics of *C. salexigens* are essentially equal at 20 and 40 °C (Fig. 5d).

In general, ectoine release is increased at higher temperatures of hypo-osmotic stress (Fig. 5e, f). For example, at 60 °C, and $<100 \text{ g L}^{-1}$ NaCl, *A. haloalkaliphilus* released its entire ectoine content. Furthermore, extracellular ectoine was detected under iso-osmotic conditions (132 g L^{-1} NaCl) in both bacteria, suggesting cell lysis or reduced membrane integrity. At this temperature, *C. salexigens* secreted almost all of its ectoine at all salinities (Fig. 5f). Large differences in ectoine content (up to 25 %) were found between treated and untreated cells, possibly attributable to the washing step before osmotic treatment. In addition, the cells might have metabolized some intracellular ectoine during pre-heating of the cell pellets. Nonetheless, the ectoine release trends are distinguishable and significant.

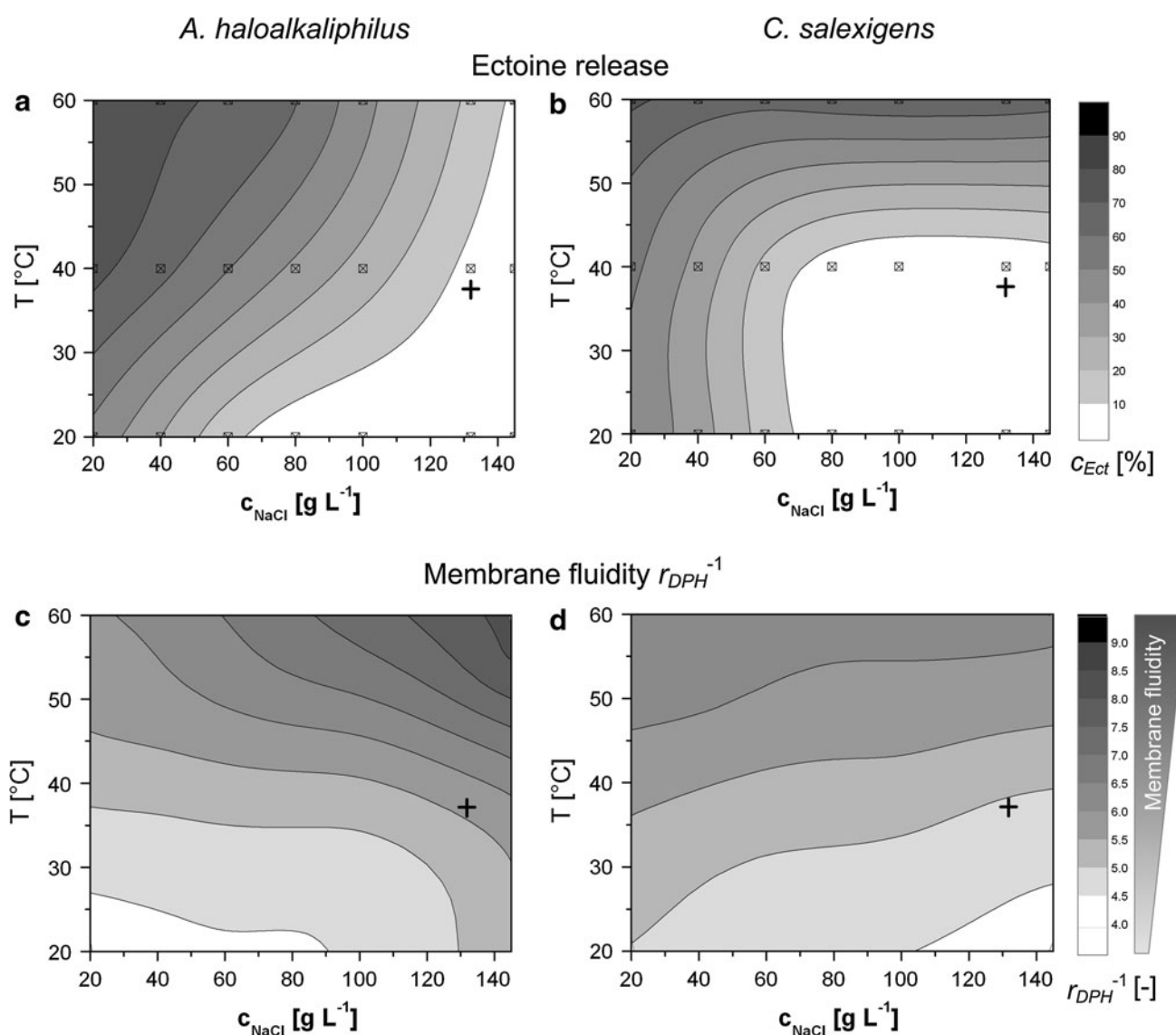


Fig. 6 Trends of ectoine release (a, b) and membrane fluidity r_{DPH}^{-1} of DPH-labeled cells (c, d) in response to temperature and salinity. The cells were grown at 37 °C in nutrient broth containing 132 g L^{-1}

NaCl (cross symbol) and subsequently shocked. The figure summarizes the data from Figs. 2 and 4, and provides a uniform presentation within the experimental range

Comparing both organisms, *A. haloalkaliphilus* is able to secrete ectoine already under weak hypo-osmotic shock conditions (80 and 100 g L⁻¹ NaCl). Surprisingly, the membrane fluidity of *A. haloalkaliphilus* under these stress conditions was lower than that of *C. salexigens* (compare Fig. 3a, b), prompting a detailed analysis of the membrane fluidity in terms of ectoine release.

Membrane fluidity and ectoine release

The relationship between ectoine release and membrane fluidity under temperature and salinity stress is deduced from the results of Figs. 3 and 4. The general ectoine discharge trends are quite similar for both bacteria, given the reduced osmotic “resistance” of *A. haloalkaliphilus* cells at higher temperature (Fig. 6a, b). The membrane fluidity r_{DPH}^{-1} of the two species shows opposite behavior within the investigated experimental range (Fig. 6c, d). For both bacteria, typical of lipid bilayers, the increase in r_{DPH}^{-1} is strongly driven by temperature. In *A. haloalkaliphilus*, this temperature effect occurs mainly above 40 °C. Below 40 °C, the membrane fluidity is affected by osmotic

downshock (Fig. 6c). On the other hand, the membrane fluidity of *C. salexigens* cells is almost unaffected by osmotic treatment (Fig. 6d). In general, higher temperatures increase the membrane fluidity and encourage ectoine release. However, *A. haloalkaliphilus* is significantly influenced by osmotic treatment. Since *C. salexigens* cell membranes are more fluid at 60 °C for all investigated shocks, *C. salexigens* has likely undergone cell damage (Fig. 6b, d).

Membrane integrity

The proportion of cells with reduced membrane integrity (expressed as disintegrated cells) during osmotic shock was assessed at several temperatures by flow cytometry. Very little cell damage occurs at 20 and 40 °C (Fig. 7a, b). At these temperatures, the membrane is a more rigid, gel-like structure (compare Fig. 6c, d). However, under hypo-osmotic treatment (reduction from 132 to 20 g L⁻¹ NaCl) about 20 % of *A. haloalkaliphilus* cells are injured. The percentage of disintegrated cells increases markedly at 40 and 60 °C with NaCl <60 g L⁻¹ (Fig. 7a). While high

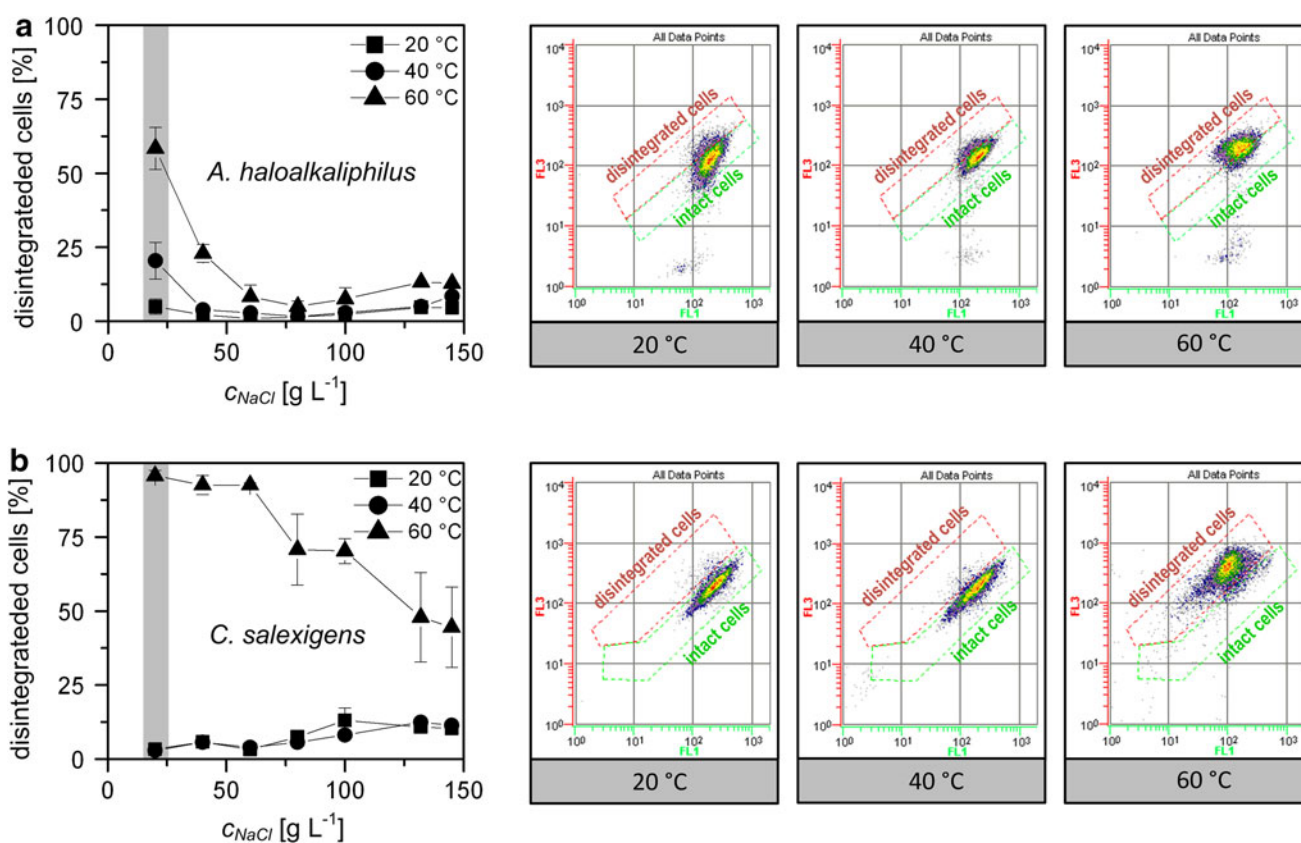


Fig. 7 Percentage of cells with reduced membrane integrity following coupled thermal and osmotic treatments. *A. haloalkaliphilus* (a), *C. salexigens* (b). As examples of the distribution of Syto 9 and PI labeled cells (fluorescing green (FL1) and red (FL3), respectively),

flow cytometric histograms (right) are shown for the gray shaded values (downshock to 20 g L⁻¹ NaCl). Disintegrated cells are delineated by the red framed regions (color figure online)

temperature per se does not adversely affect cell membrane, the combination of temperature and osmotic shocks overwhelms the bacterial resistance. On the other hand, *C. salexigens* cannot withstand 60 °C and its membrane integrity is severely reduced (Fig. 7b). This finding could explain why *C. salexigens* releases almost all of its ectoine at 60 °C, regardless of salinity (compare Fig. 5f). About 50 % of *C. salexigens* cells show reduced integrity under isosmotic conditions (132 g L⁻¹ NaCl) (Fig. 7b). Although intact cells exist, shocking to 60 °C and 20 g L⁻¹ NaCl are equivalent, in terms of quantity of ectoine secreted (Fig. 5f). At this temperature, the cell membrane state is essentially liquid-crystalline. The phase transition temperature T_m was estimated at around 40 °C (see Fig. 4). Despite the similar T_m , the percentage of *A. haloalkaliphilus* cells with reduced membrane integrity at 60 °C is comparatively low. Denaturation of membrane proteins is also possible at this temperature. Measurements conducted at salinities >100 g L⁻¹ NaCl erroneously show that around 10 % of cells are disintegrated (Fig. 7), due to the fluorescence shifts at higher saline buffer concentrations and the overlapping of living and dead cells during measurement. During method alignment, at least 8 % of exponential phase cells were labeled as disintegrated. Examples of flow cytometric histograms (Fig. 7a, b, right column) are shown for cells treated at 20, 40, and 60 °C in 20 g L⁻¹ NaCl. At 20 °C, nearly all detected cells are in the (green) fluorescence region, indicating intact cells. As temperature is raised, increasing numbers of disintegrated cells (red) with reduced membrane integrity appear. These sample heterogeneities and the associated leakage of intracellular hydrophobic compounds affect the DPH steady-state anisotropy. This method provides a harmonized measurement result, which needs to be considered when interpreting membrane fluidity changes.

Consequences of thermal and osmotic treatment on ectoine secretion

Ectoine can be released from bacterial cultures via two ways. First, the cellular membrane can be disintegrated, discharging the ectoine into the supernatant together with other proteinogenic intracellular compounds. To achieve this in *C. salexigens*, the cell suspensions can be heated to around 60 °C, when almost all the ectoine is found in the supernatant. On the other hand, *A. haloalkaliphilus* can withstand considerably higher osmotic and thermal stress. Even under drastic stress conditions ($c_{\text{NaCl}} = 20 \text{ g L}^{-1}$, $T = 60 \text{ °C}$) membrane integrity disrupted in only 58 % of the cells. However, the compatible solute ectoine can be extracted from cells without disrupting their membrane integrity and viability. Such a procedure would simplify downstream processes and preserve the cells for continued

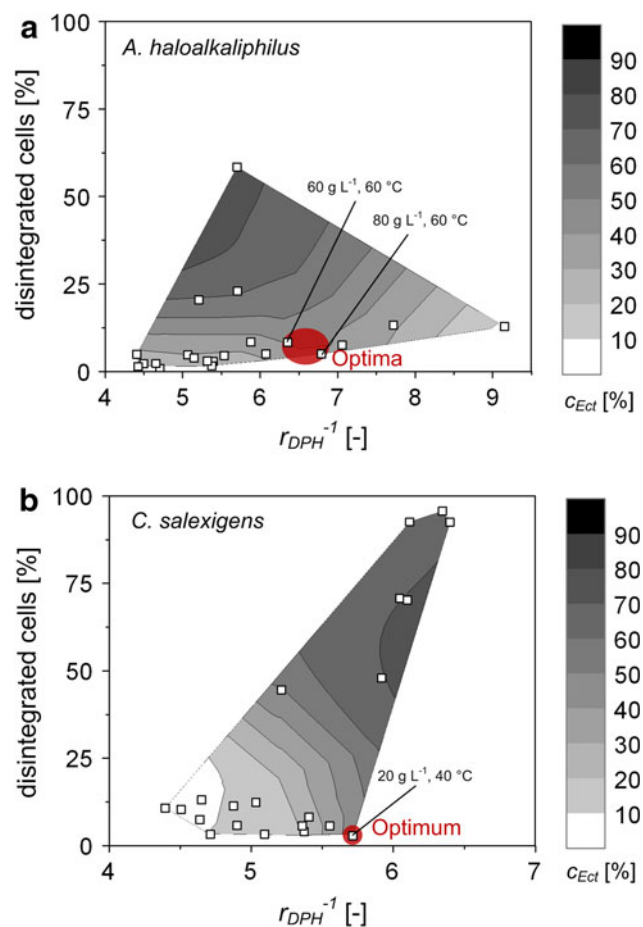


Fig. 8 Determination of optimal ectoine secretion conditions (high ectoine secretion with preserved membrane integrity) for *A. haloalkaliphilus* (a), and *C. salexigens* (b)

ectoine synthesis (the principle of the so-called “bacterial milking”). To estimate the viability of this scheme, the membrane properties fluidity and integrity can be related to ectoine release. The conditions for optimally efficient bacterial milking are different for the two strains. In *A. haloalkaliphilus*, optimal ectoine secretion at 60 °C occurs under hypo-osmotic stress at 60–80 g L⁻¹ NaCl (Fig. 8a), whereas *C. salexigens* cells should be shocked from 132 to 20 g L⁻¹ NaCl at a lower temperature (about 40 °C; Fig. 8b). Under these conditions, extracellular ectoine concentration is high while the membrane integrity remains largely intact. In both cases, the membrane fluidity is slightly enhanced, suggesting that a flexible membrane structure is beneficial for optimal ectoine release.

Conclusions

Ectoine release of the halophilic bacteria *A. haloalkaliphilus* and *C. salexigens* was induced by an osmotic gradient and temperature increase. Shocking at higher temperatures

reduced the membrane integrity and increased membrane fluidity.

A certain temperature might be beneficial to generate a minimum membrane fluidity for ectoine release. However, the consequence of temperature and osmotic treatment, such as bacterial osmoregulation and lysis, appear more crucial to ectoine release. During osmotic downshock, mechanosensitive channels release ectoine by creating large pores within cellular membrane. Such openings distort and shrink the cell wall, thereby affecting the fluidity of the lipid bilayers. However, since the mechanosensitive channels should still be closed at the time of DPH steady-state measurements (20–40 min after osmotic downshock), this phenomenon cannot explain the membrane fluidity changes in this study. In addition, sample heterogeneities due to cell lysis and leaked intracellular hydrophobic compounds influence the DPH steady-state anisotropy, which is an overall sample measure. In these terms, it is concluded that the membrane fluidity of *A. haloalkaliphilus* is affected by osmotic downshock and temperature, whereas that of *C. salexigens* is degraded chiefly by temperature. Different cell wall structure and membrane compounds, as well as modifications of fatty acids, might explain the opposite trends observed in the two bacteria. In addition, the unequal environmental conditions (pH) may affect the charges on phosphate head groups, with consequent effects on lipid bilayer fluidity. Surprisingly, the cellular membrane of *A. haloalkaliphilus* became more fluid as salinity increases under isothermal conditions. This adjustment to high salinity may enhance the transport capability of the organism.

In summary, membrane fluidity measurements using DPH steady-state anisotropy can appropriately detect changes in the membrane fluidity of halophiles. Heterogeneities developing in stressed cultures, and prolonged incubation times, are impediments to stress investigations. Nevertheless, in this study of two bacterial species exposed to osmotic and temperature stress, valuable qualitative interpretations and interesting properties of membrane fluidity changes have been investigated. The ectoine secretion capacity of *A. haloalkaliphilus* and *C. salexigens* differ with respect to membrane properties, thermal resistance and response to osmotic and thermal stress. With regard to “bacterial milking”, stress conditions have been identified that ensure high ectoine secretion, while preserving the cellular integrity of the producing microorganisms.

Acknowledgments The authors gratefully acknowledge the financial support granted by the German Research Foundation (DFG), No. FR 2596/2-1.

Conflict of interest The authors have declared no conflict of interest.

References

1. Harishchandra RK, Wulff S, Lentzen G, Neuhaus T, Galla H-J (2010) The effect of compatible solute ectoines on the structural organization of lipid monolayer and bilayer membranes. *Biophys Chem* 150(1–3):37–46
2. Oren A (2002) Halophilic microorganisms and their environments. Kluwer Academic Publishers, New York
3. Russell NJ (1989) Adaptive modifications in membranes of halotolerant and halophilic microorganisms. *J Bioenerg Biomembr* 21(1):93–113
4. Simonin H, Beney L, Gervais P (2008) Controlling the membrane fluidity of yeasts during coupled thermal and osmotic treatments. *Biotechnol Bioeng* 100(2):325–333
5. Laroche C, Beney L, Marechal PA, Gervais P (2001) The effect of osmotic pressure on the membrane fluidity of *Saccharomyces cerevisiae* at different physiological temperatures. *Appl Microbiol Biotechnol* 56(1–2):249–254
6. Beney L, Mille Y, Gervais P (2004) Death of *Escherichia coli* during rapid and severe dehydration is related to lipid phase transition. *Appl Microbiol Biotechnol* 65(4):457–464
7. Lakowicz JR (2006) Principles of fluorescence spectroscopy, 3rd edn. Springer, New York
8. Lentz BR (1993) Use of fluorescent probes to monitor molecular order and motions within liposome bilayers. *Chem Phys Lipids* 64(1–3):99–116
9. Petty HR, Niebylski CD, Francis JW (1987) Influence of immune complexes on macrophage membrane fluidity: a nanosecond fluorescence anisotropy study. *Biochemistry* 26(20):6340–6348
10. Vincent M, England LS, Trevors JT (2004) Cytoplasmic membrane polarization in Gram-positive and Gram-negative bacteria grown in the absence and presence of tetracycline. *Biochim Biophys Acta* 1672(3):131–134
11. Myktyczuk NCS, Trevors JT, Leduc LG, Ferroni GD (2007) Fluorescence polarization in studies of bacterial cytoplasmic membrane fluidity under environmental stress. *Prog Biophys Mol Biol* 95(1–3):60–82
12. Hosono K (1992) Effect of salt stress on lipid composition and membrane fluidity of the salttolerant yeast *Zygosaccharomyces rouxii*. *J Gen Microbiol* 138(1):91–96
13. Nichols DS, Olley J, Garda H, Brenner RR, McMeekin TA (2000) Effect of temperature and salinity stress on growth and lipid composition of *Shewanella gelidimarina*. *Appl Environ Microbiol* 66(6):2422–2429
14. López CS, Garda HA, Rivas EA (2002) The effect of osmotic stress on the biophysical behavior of the *Bacillus subtilis* membrane studied by dynamic and steady-state fluorescence anisotropy. *Arch Biochem Biophys* 408(2):220–228
15. Tymczyszyn EE, Gómez-Zavaglia A, Disalvo EA (2005) Influence of the growth at high osmolality on the lipid composition, water permeability and osmotic response of *Lactobacillus bulgaricus*. *Arch Biochem Biophys* 443(1–2):66–73
16. Huffer S, Clark ME, Ning JC, Blanch HW, Clark DS (2011) Role of alcohols in growth, lipid composition, and membrane fluidity of yeasts, bacteria, and archaea. *Appl Environ Microbiol* 77(18):6400–6408
17. Mueller S, Ullrich S, Loesche A, Loffhagen N, Babel W (2000) Flow cytometric techniques to characterize physiological states of *Acinetobacter calcoaceticus*. *J Microbiol Methods* 40(1):67–77
18. Shapiro HM (2003) Practical flow cytometry, 4th edn. Wiley, New York
19. Mueller S, Nebe-von-Caron G (2010) Functional single-cell analyses: flow cytometry and cell sorting of microbial populations and communities. *FEMS Microbiol Rev* 34(4):554–587

20. Bergmann S, David F, Franco-Lara E, Wittmann C, Krull R (2013) Ectoine production by *Alkalibacillus haloalkaliphilus*—bioprocess development using response surface methodology and model-driven strategies. *Eng Life Sci* 13 (in press)
21. Fallet C, Rohe P, Franco-Lara E (2010) Process optimization of the integrated synthesis and secretion of ectoine and hydroxyectoine under hyper/hypo-osmotic stress. *Biotechnol Bioeng* 107(1):124–133
22. Bligh EG, Dyer WJ (1959) A rapid method of total lipid extraction and purification. *Can J Biochem Physiol* 37(8):911–917
23. Marangoni AG, Narine SS (2002) *Physical properties of lipids*. Marcel Dekker, New York
24. Fritze D (1996) *Bacillus haloalkaliphilus* sp. nov. *Int J Syst Bacteriol* 46(1):98–101
25. Jeon CO, Lim J-M, Lee J-M, Xu L-H, Jiang C-L, Kim C-J (2005) Reclassification of *Bacillus haloalkaliphilus* Fritze 1996 as *Alkalibacillus haloalkaliphilus* gen. nov., comb. nov. and the description of *Alkalibacillus salilacus* sp. nov., a novel halophilic bacterium isolated from a salt lake in China. *Int J Syst Evol Microbiol* 55(Pt 5):1891–1896
26. Sauer T, Galinski EA (1998) Bacterial milking: a novel bioprocess for production of compatible solutes. *Biotechnol Bioeng* 57(3):306–313
27. Pastor JM, Salvador M, Argandoña M, Bernal V, Reina-Bueno M, Csonka LN, Iborra JL, Vargas C, Nieto JJ, Cánovas M (2010) Ectoines in cell stress protection: uses and biotechnological production. *Biotechnol Adv* 28(6):782–801
28. Clejan S, Krulwich TA, Mondrus KR, Seto-Young D (1986) Membrane lipid composition of obligately and facultatively alkaliphilic strains of *Bacillus* spp. *J Bacteriol* 168(1):334–340
29. Yumoto I (2002) Bioenergetics of alkaliphilic *Bacillus* spp. *J Biosci Bioeng* 93(4):342–353
30. Beney L, Simonin H, Mille Y, Gervais P (2007) Membrane physical state as key parameter for the resistance of the gram-negative *Bradyrhizobium japonicum* to hyperosmotic treatments. *Arch Microbiol* 187(5):387–396
31. Träuble H, Teubner M, Woolley P, Eibl H (1976) Electrostatic interactions at charged lipid membranes. *Biophys Chem* 4(4):319–342
32. Vargas C, Kallimanis A, Koukkou AI, Calderon MI, Canovas D, Iglesias-Guerra F, Drainas C, Ventosa A, Nieto JJ (2005) Contribution of chemical changes in membrane lipids to the osmoadaptation of the halophilic bacterium *Chromohalobacter salexigens*. *Syst Appl Microbiol* 28(7):571–581
33. Ventosa A (2004) *Halophilic microorganisms*. Springer, Berlin